Journal of Solid State Chemistry 182 (2009) 2208–2212

Contents lists available at ScienceDirect

Journal of Solid State Chemistry

journal homepage: www.elsevier.com/locate/jssc

Hydrothermal syntheses, structures, and magnetic properties of $(NH_4)_2NaVF_6$ and Na_3VF_6

Lijie He, Hongming Yuan, Keke Huang, Chen Yan, Guanghua Li, Qiaoru He, Yang Yu, Shouhua Feng *

State Key Laboratory of Inorganic Synthesis and Preparative Chemistry, College of Chemistry, Jilin University, Changchun 130012, PR China

ARTICLE INFO

Article history:
Received 10 February 2009
Received in revised form
24 March 2009
Accepted 29 March 2009
Available online 8 April 2009

Keywords:
Hydrothermal
Perovskite
Fluoride
Magnetic property

ABSTRACT

The single crystals of perovskite fluorides $(NH_4)_2NaVF_6$ and Na_3VF_6 were synthesized under mild hydrothermal conditions. The structures of the compounds were determined by means of single-crystal and powder X-ray diffraction analyses, respectively. $(NH_4)_2NaVF_6$ has a cubic elpasolite-type structure and crystallizes in the space group $Fm\bar{3}m$ with lattice constant $a = 8.495(0)$ Å. Rietveld refinement indicates that Na_3VF_6 has a monoclinic structure and is in space group $P2_1/n$. The compounds were characterized by scanning electron microscopy, thermogravimetric and differential thermal analysis, and variable temperature magnetic susceptibility. With the temperature decreasing, the magnetic studies of the compounds showed the magnetic ordering was related to the crystallographic features and isolated magnetic units.

1. Introduction

A large family of $A_2BB'F_6$ type elpasolite and $A_3B'F_6$ type cryolite (A, B = Li, Na, K, Rb, Tl, NH_4, and B' = Al, Sc, V, Cr, Fe, Bi, Ga, Y, In, Ln) is extensively investigated due to the interesting structural phase transition at low temperature [1–4] and remarkable features for acting as host materials for luminescent ions due to their wide range of wavelength transmission and low refractive index [5]. Alter et al. used the conventional solid state method to synthesize the cryolite-type Na_3VF_6 (space group $P21/n$, $a = 5.51(3)$ Å, $b = 5.72(1)$ Å and $c = 7.69(3)$ Å) which is isotypic with cryolite Na_3AlF_6 [6]. Massa et al. synthesized the elpasolite-type compound of $(NH_4)_2NaVF_6$ at 700 °C in a platinum tube sealed under an inert atmosphere [7]. But the magnetic property of $(NH_4)_2NaVF_6$ was not investigated. It is well known that the inorganic frameworks of cryolite and elpasolite are mainly the perovskite structures of which there are two kinds of non-equivalent octahedral groups BF_6 and $B'F_6$ with different charge and these octahedral alternate along the three four-fold crystal axes. Their phase stabilities are governed by the tolerance factor t in terms of the sizes of A, B and B' cations [3], $t = \sqrt{2}(R_A+R_X)/(R_B+R_{B'}+2R_X)$, where R_A, R_B, $R_{B'}$ and R_X are the ionic radii of the corresponding ions in the general formula.

Besides the structural studies, many methods were applied to the preparation of the fluorides such as solid-state reaction [8–10], sol–gel precursors [11–14], flux growth [15,16], hydrothermal process [17–21] and fused-salt electrolysis method [22]. Among them, the hydrothermal method provides an attractive alternative for the synthesis of materials that would usually be prepared with the traditional high temperature solid-state methods [23–25]. The use of a solvent in hydrothermal synthesis, carried out under relatively mild conditions, would permit a rapid mixing of several chemical elements, leading to homogeneous products with controllable particle size, which is rather difficult to achieve when using the high temperature solid-state technique. The mild hydrothermal conditions are also desirable in the preparation for crystals of rare earth and complex fluorides since they have the advantages such as low temperature requirement, one-step synthetic procedure, easy handling and controllable particle size distribution. Under the mild hydrothermal condition, complex fluorides, such as perovskite-type fluorides $LiBaF_3$, $KMgF_3$ and the scheelite-type fluorides $LiYF_4$, $NaYF_4$, KYF_4 and $BaBeF_4$, were synthesized by our research group. We also investigated the luminescence of lanthanide doping of these compounds [26,27]. As an extension of our study, we present the hydrothermal syntheses, structural characterization and magnetic studies of double perovskite vanadium fluorides $(NH_4)_2NaVF_6$ and Na_3VF_6.

2. Experimental section

Single crystals of title compounds were synthesized from a mixture of NH_4HF_2, NaF, V_2O_3, HF acid and water. A typical synthesis process of $(NH_4)_2NaVF_6$ was the mixture of 0.799 g NH_4HF_2, 0.042 g NaF, 0.124 g $Na_2S_2O_3$, 0.075 g V_2O_3, 2.0 mL HF acid

* Corresponding author. Fax: +86 431 85168624.
E-mail address: shfeng@mail.jlu.edu.cn (S. Feng).

0022-4596/$ - see front matter © 2009 Elsevier Inc. All rights reserved.
doi:10.1016/j.jssc.2009.03.024

Table 1
Crystallographic and chemical data of $(NH_4)_2NaVF_6$.

Chemical formula	$N_2H_8F_6NaV$
Formula weight ($g\,mol^{-1}$)	224.01
Temperature (K)	298 (2)
Wavelength (Å)	0.71073
Crystal system	Cubic
Space group	$Fm\bar{3}m$ (no. 225)
Crystal size	$0.20\times0.20\times0.20$ mm
a (Å)	8.5001(2)
Z	4
Volume	614.15(3) $Å^3$
Calculated density ($Mg\,m^{-3}$)	2.423
Absorption coefficient (mm^{-1})	1.738
F [000]	440
θ range (deg)	4.15–33.25
Reflections collected/unique	1438/88
Data/restraints/parameters	88/1/9
Goodness-of-fit on F^2	1.053
Final R indices ($I>2\sigma(I)$)	$R_1=0.0174$
	$wR_2=0.0692$
R indices (all data)	$R_1=0.0177$
	$wR_2=0.0695$
Largest diff. peak and hole ($e/Å^{-3}$)	0.190 and −0.308

Table 2
Atomic coordinates ($\times10^4$) and equivalent isotropic displacement parameters ($Å^2\times10^3$) for $(NH_4)_2NaVF_6$.

	x	y	z	U(eq)
V(1)	0	0	5000	12(1)
Na(1)	0	−5000	5000	15(1)
F(1)	0	−2267(2)	5000	25(1)
N(1)	2500	2500	2500	19(1)

Table 3
Selected bond lengths and angles (Å, deg) for $(NH_4)_2NaVF_6$.

V(1)–F(1)♯1	1.9350(18)	Na(1)–F(1)	2.3150(18)
V(1)–F(1)♯2	1.9350(18)	Na(1)–F(1)♯6	2.3150(18)
V(1)–F(1)♯3	1.9350(18)	Na(1)–F(1)♯7	2.3150(18)
V(1)–F(1)♯4	1.9350(18)	Na(1)–F(1)♯8	2.3150(18)
V(1)–F(1)	1.9350(18)	Na(1)–F(1)♯9	2.3150(18)
V(1)–F(1)♯5	1.9350(18)	Na(1)–F(1)♯10	2.3150(18)
N(1)–H(1)	0.92(2)		
F(1)♯1–V(1)–F(1)	90.0	F(1)♯6–Na(1)–F(1)	90.0
F(1)♯1–V(1)–F(1)♯2	90.0	F(1)♯7–Na(1)–F(1)	90.0
F(1)–V(1)–F(1)♯2	90.0	F(1)♯6–Na(1)–F(1)♯8	90.0
F(1)♯1–V(1)–F(1)♯3	90.0	F(1)♯7–Na(1)–F(1)♯8	90.0
F(1)♯2–V(1)–F(1)♯3	90.0	F(1)–Na(1)–F(1)♯8	90.0
F(1)♯1–V(1)–F(1)♯4	180.0	F(1)♯6–Na(1)–F(1)♯9	90.0
F(1)–V(1)–F(1)♯4	90.0	F(1)♯7–Na(1)–F(1)♯9	90.0
F(1)♯2–V(1)–F(1)♯4	90.0	F(1)–Na(1)–F(1)♯9	90.0
F(1)♯3–V(1)–F(1)♯4	90.0	F(1)♯8–Na(1)–F(1)♯9	180.0
F(1)–V(1)–F(1)♯5	90.0	F(1)♯6–Na(1)–F(1)♯10	90.0
F(1)♯2–V(1)–F(1)♯5	180.0	F(1)♯7–Na(1)–F(1)♯10	90.0
F(1)♯3–V(1)–F(1)♯5	90.0	F(1)–Na(1)–F(1)♯10	180.0
F(1)♯4–V(1)–F(1)♯5	90.0	F(1)♯8–Na(1)–F(1)♯10	90.0
F(1)♯6–Na(1)–F(1)♯7	180.0	F(1)♯9–Na(1)–F(1)♯10	90.0
F(1)♯6–Na(1)–F(1)	90.0	V(1)–F(1)–Na(1)	180.0

Symmetry transformations used to generate equivalent atoms: ♯1: $-z+1/2, -x, -y+1/2$; ♯2: $-y, -z+1/2, -x+1/2$; ♯3: $-x,-y,-z+1$; ♯4: $z-1/2, x, y+1/2$; ♯5: $y, z-1/2, x+1/2$; ♯6: $-y-1/2, -z, -x+1/2$; ♯7: $y+1/2, z-1, x+1/2$; ♯8: $z-1/2, x-1/2, y+1$; ♯9: $-z+1/2, -x-1/2, -y$; ♯10: $-x, -y-1, -z+1$.

with 8.5 mL deionized water. After magnetic stirring for about 10 min at room temperature, the mixture was sealed in a 11 mL Teflon-lined stainless-steel autoclave with a filling capacity of about 80% at 180 °C for 3 days. Finally the autoclave was cooled and depressurized, and the crystalline products were washed with distilled water and dried in air at ambient temperature. The preparation of Na_3VF_6 began with mixing 0.075 g V_2O_3, 0.126 g NaF and 7.0 mL deionized water, and 2.0 mL HF acid were subsequently mixed to form a mixture. The crystallization process is the same as used for $(NH_4)_2NaVF_6$.

The composition of samples is determined by EDX (AXIOS PANAlytical). The contents of nitrogen and hydrogen in the compounds are measured by elemental analyzer (a Perkin-Elmer 2400).

The powder X-ray diffraction (XRD) data were collected using a Rigaku D/Max 2550V/PC X-ray diffractometer with Cu$K\alpha$ radiation ($\lambda=1.5418$ Å) of 40 KV and 200 mA at room temperature by step scanning in the angle range $5^\circ\leqslant2\theta\leqslant80^\circ$ with increments of 0.02°. Scanning electron microscopy (SEM) was performed with a Rigaku JSM-6700 F microscope operated at 10 kV. The magnetic susceptibilities were measured with a SQUID magnetometer (Quantum Design, MPMS-LX) at field-cooled and zero-field-cooled experiments and temperature in the range 4–300 K. The single crystal X-ray investigation was performed on a Siemens SMART CCD diffractometer with graphite-monochromated Mo$K\alpha$ ($\lambda=0.71073$ Å) radiation at a temperature of 298 ± 2 K. A hemisphere of data were collected using a narrow-frame method with scan widths of 0.30° in ω and an exposure time of 30 s/frame. Data processing was accomplished with the SAINT processing program [28], using the SHELXTL crystallographic software package [29]. All data collection conditions of $(NH_4)_2NaVF_6$ are reported in Table 1. Table 2 provides the atomic coordinates and equivalent isotropic displacement parameters. The selected bond length (Å) and angles (deg) are listed in Table 3.

3. Results and discussion

The pH value, appropriate reaction temperature and pressure range play important roles for crystalline materials in experimental duration. In our cases, it has been found that the title compounds cannot be obtained when reaction temperature is lower than 180 °C and pH value in solution is higher than 4. The addition amount of NH_4HF_2 is likely a key factor to the formation of $(NH_4)_2NaVF_6$. NH_4HF_2 provides the sources of NH_4^+ and F^-, but the pH buffer for the reaction system. $Na_2S_2O_3$ as reducing agent stabilized the oxidation sate of V^{3+} in the solution. Without the reducing agent, we obtained impurity of blue crystal of $(NH_4)_2NaVOF_5$, where V^{3+} was oxidized into V^{4+}.

Single crystal of $(NH_4)_2NaVF_6$ is suitable for single-crystal X-ray structural analysis was confirmed by SEM image as shown in Fig. 1(a). The crystal structure of the compound consists of three-dimension nets built up from vertex-sharing strictly alternating NaF_6 and VF_6 octahedra, which is isostructural with elpasolite K_2NaAlF_6 (Fig. 2). Vanadium and sodium atoms occupy same crystallographic independent position in the asymmetric unit. The vanadium atom shares six fluorine atoms with adjacent sodium atoms shown in Fig. 3. The V–F, Na–F and N–H bond lengths are 1.917(3), 2.330(3) and 0.92(2) Å, respectively, being longer than that usually observed for V–F and Na–F distances in Na_3VF_6 reported earlier [6]. All of F–V–F and F–Na–F bond angles are 180°. The volume of VF_6 octahedron is smaller than that of NaF_6 octahedron. Each of NH_4^+ ions is surrounded by 12 F^- ions. In the $A_2BB'F_6$ type elpasolite, changes in the ratio of the sizes of the A type cations may result in tilting or rotating of the BF_6 octahedra, lowering their symmetry. For example, $(NH_4)_2NaVF_6$ is cubic at room temperature but replaces the two NH_4 cations with Na to give

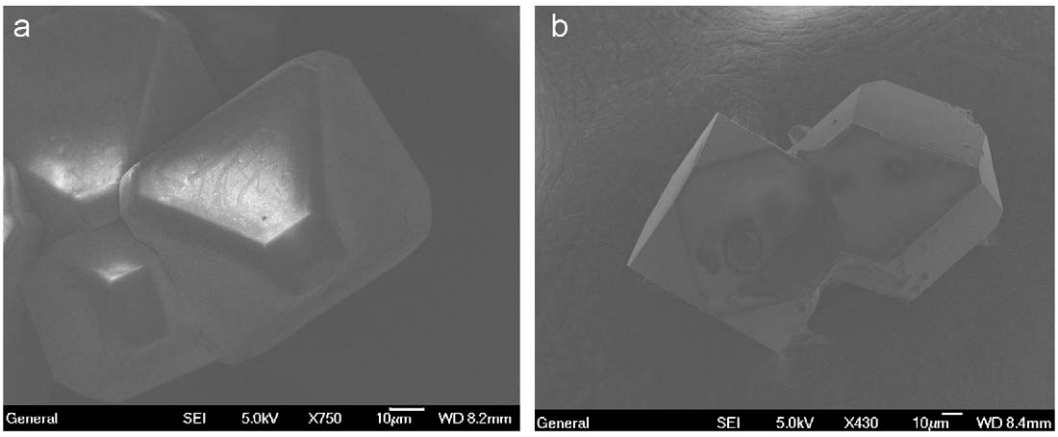

Fig. 1. SEM images of $(NH_4)_2NaVF_6$ (a) and Na_3VF_6 (b).

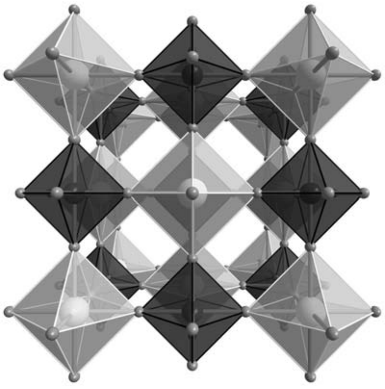

Fig. 2. Perspective view of the $(NH_4)_2NaVF_6$ elpasolite structure (sodium octahedra are light gray and vanadium octahedra dark gray, ammonium are omitted for clarity).

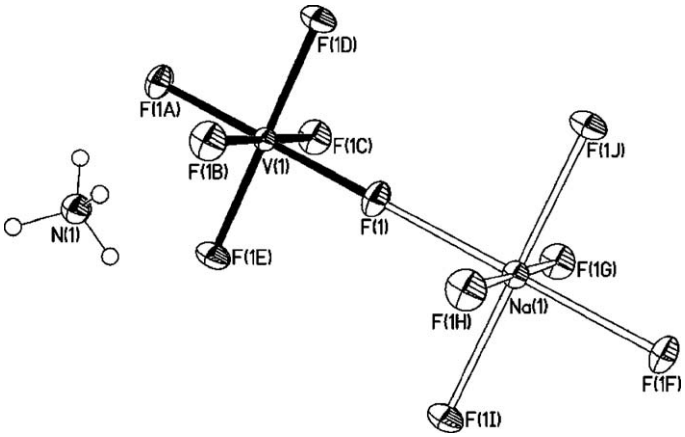

Fig. 3. ORTEP drawing of the coordination environments of the metal atoms in $(NH_4)_2NaVF_6$.

cryolite Na_3VF_6. The differences in the structures between the two compounds are due to different radii of *A* type cations.

The room-temperature powder XRD pattern of Na_3VF_6 is shown in Fig. 4. The structure was refined with the Rietveld method and the atomic positions were are in Table 4. The powder XRD pattern was well indexed in a monoclinic unit cell of space group $P2_1/n$ with lattice parameters $a = 5.510(6)$ Å, $b = 5.725(8)$ Å, $c = 7.948(6)$ Å and $\beta = 90.410(8)^\circ$, which is identical with that previously reported (ICDD-PDF 26–1493).

TG/DTA curves of $(NH_4)_2NaVF_6$ and Na_3VF_6 were measured from 25 to 400 °C in N_2 with a heating rate of 10 °C min^{-1} as shown in Fig. 5. As shown in Fig. 5a, there was endothermic peak located at about 350 °C in the DTA curve for $(NH_4)_2NaVF_6$. Correspondingly there was a continual weight loss of 33.76% in the temperature range 300–350 °C in the TG curve. The compound was stable up to 300 °C, and then it started to decompose. In comparison of $(NH_4)_2NaVF_6$, Na_3VF_6 was stable when the temperature increased up to 400 °C as shown in Fig. 5b.

The different arrangement of MF_6 octahedra results in the formation of a variety of one-dimensional chain, two-dimensional layer, three-dimensional framework structures and isolated unit in fluorides. Their magnetic behavior is related to crystallographic features since electrons are localized strongly [30]. The variation of the molar magnetic susceptibilities χ_M of $(NH_4)_2NaVF_6$ and Na_3VF_6 were investigated in temperature range 4–300 K in 5 and 1 K Oe applied field, respectively. The results are shown as plots of χ_M^{-1} versus T in Fig. 6. Their magnetic behavior in the range of higher temperature obeys the Curie–Weiss law $\chi = C/(T-\theta)$ with $C = 0.9256\ cm^3\ K\ mol^{-1}$, $\theta = -52$ K for $(NH_4)_2NaVF_6$ and

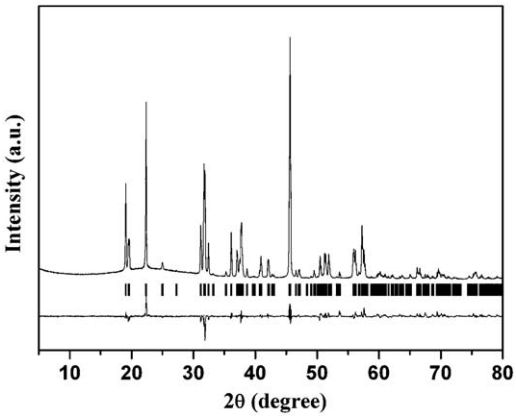

Fig. 4. Rietveld refinement of Na_3VF_6 ($R_{wp} = 9.95\%$, $R_p = 6.39\%$). Observed (dotted line) and calculated (solid line) X-ray diffraction patterns are shown on top. The difference between observed and calculated intensities is shown as difference plot on the bottom. The vertical bars are the Bragg positions of the reflection (tick marks) are also shown.

$C = 1\ cm^3\ K\ mol^{-1}$, $\theta = -63$ K for Na_3VF_6, respectively. The negative Weiss constants mean that there is antiferromagnetic interaction between V^{3+} cations in these compounds. The effective moment μ_{eff} for compound $(NH_4)_2NaVF_6$ was calculated to be $2.72\mu_{eff}/\mu_B$ by fitting the χ_M^{-1} versus T curve at higher temperature zone, which is very close to the value of spin-only state V^{3+}

Table 4
Atom positions and the reliability factors for the Rietveld refinements of Na_3VF_6 from XRD data.

Atom	*x*	*y*	*z*
V	0	0	0
Na1	0	0	0.5
Na2	−0.0060(8)	0.4448(2)	0.2586(9)
F1	0.0826(6)	0.2987(5)	−0.0130(1)
F2	0.0843(7)	0.0913(8)	0.2175(9)
F3	0.8078(7)	0.6298(4)	0.4942(0)

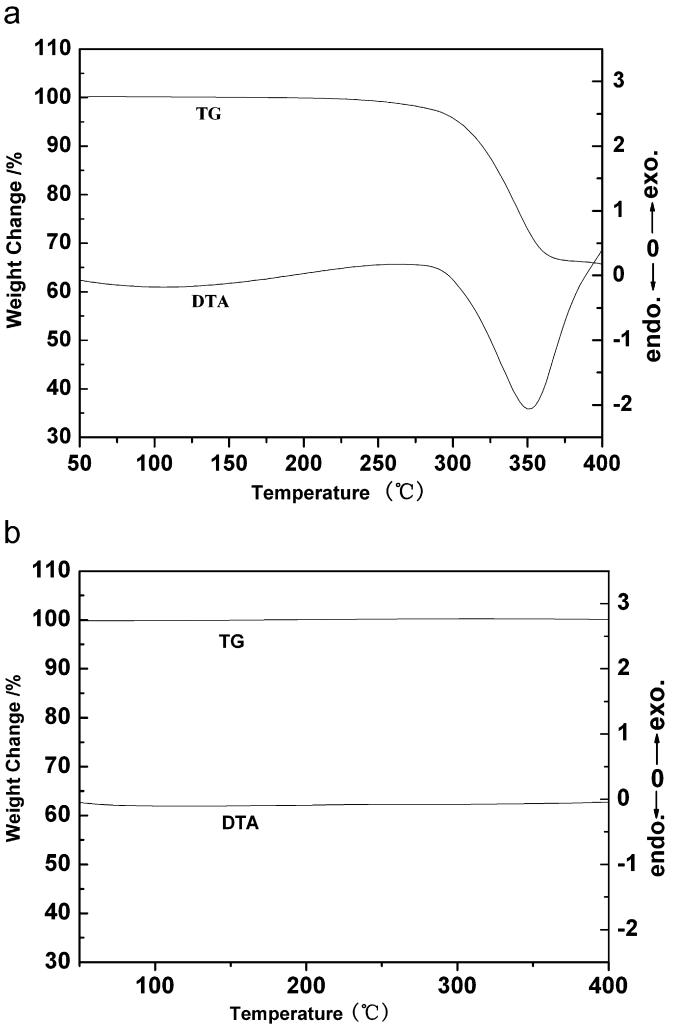

Fig. 5. TG–DTA curves in N_2 of $(NH_4)_2NaVF_6$ (a) and Na_3VF_6 (b).

($2.828\mu_{eff}/\mu_B$). But μ_{eff} for Na_3VF_6 is $2.573\mu_B$ at room temperature, which is slightly lower than the value of spin-only state V^{3+}. Alter et al. have suggested that antiferromagnetism observed in VF_3 at 18 K can be explained in term of super-exchange model [6]. The VF_6 octahedra are isolated by NaF_6 octahedra in title compounds, which lead to the long distance super-exchange interactions between V^{3+} cations. Obviously, Fig. 6 shows that there are separations between the theoretically fitted lines and experimental curves compared with $(NH_4)_2NaVF_6$ at 196 K and Na_3VF_6 at 110 K, respectively. It is noticed that fluorine octahedron is a rigid unit and remains almost undistorted. Kennedy et al. claimed that the reason of lowing symmetry from cubic to monoclinic as temperature decreases is in-phase and out-of phase of AlF_6 and NaF_6 octahedra. The deviation from linearity of the

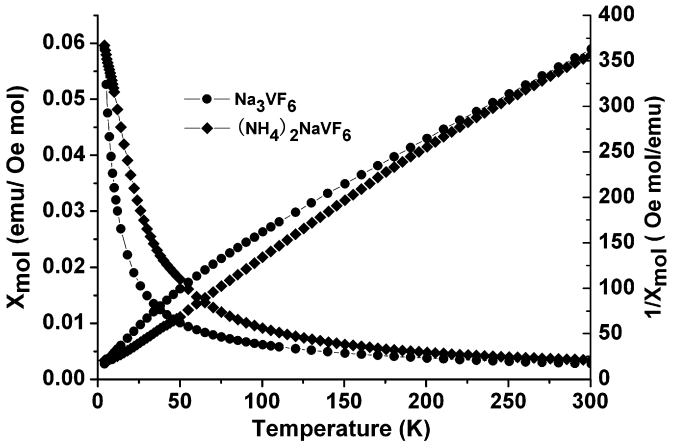

Fig. 6. The magnetization curves of $(NH_4)_2NaVF_6$ in an applied field of 5 KOe and Na_3VF_6 in an applied field of 1 KOe.

curves with decreasing temperature is probably the consequence of canting spin order of V^{3+} induced by changing crystallographic symmetry. We proposed the difference in magnetic properties between $(NH_4)_2NaVF_6$ and Na_3VF_6 were caused by the different metal–F–metal bond [31]. In the structure of $(NH_4)_2NaVF_6$, the angle of the V–F–Na is 180°. But in the structure of Na_3VF_6, the V–F–Na bond is distorted from the ideal value of 180°. As the mechanism of the super-exchange interaction between the transition metals via fluorine is changed, the magnetic property can be considered to be dramatically changed by V–F–Na bond.

4. Conclusions

Single crystals of $(NH_4)_2NaVF_6$ and Na_3VF_6 were synthesized under hydrothermal conditions. This method is advantageous due to the mild conditions required, one-step synthetic procedure and easy handling. $(NH_4)_2NaVF_6$ and Na_3VF_6 were characterized by X-ray diffraction. For their syntheses, the reactants NH_4HF_2 and $Na_2S_2O_3$ play critical roles. The compounds show the existence of canted antiferromagnetic interactions.

Acknowledgment

This work was supported by the National Science Foundation of China (nos. 20631010 and 20771042).

Appendix A. Supplementary material

Supplementary data associated with this article can be found in the online version at doi:10.1016/j.jssc.2009.03.024.

References

[1] I.N. Flerov, M.V. Gorev, J. Grannec, A. Tresaud, J. Fluorine Chem. 116 (2002) 9–14.
[2] M. Ahrens, K. Schuschke, S. Redmer, E. Kemnitz, Solid State Sci. 9 (2007) 833–837.
[3] I.N. Flerov, M.V. Gorev, K.S. Aleksandrov, A. Tressaud, J. Grannec, M. Couzi, Mat. Sci. Eng. 24 (1998) 81–85.
[4] Q.D. Zhou, B.J. Kennedy, J. Solid State Chem. 177 (2004) 654–659.
[5] E.P. Chicklis, C.S. Naiman, R.C. Folweiler, D.R. Gabbe, J.P. Jenssen, A. Linz, Appl. Phys. Lett. 19 (1971) 119.
[6] V.E. Alter, R. Hoppe, Z. Anorg, Allg. Chem. 421 (1975) 110–120.
[7] W. Massa, Z. Anorg, Allg. Chem. 427 (1976) 235–240.
[8] P.R. Slater, R.K.B. Gover, J. Mater. Chem. 11 (2001) 2035–2038.

[9] J.H. Choy, J.Y. Kim, S.J. Kim, J.S. Sohn, Chem. Mater. 13 (2001) 906–912.
[10] A. Caramanian, J.P. Souron, P. Gredin, A. de Kozak, J. Solid State Chem. 159 (2001) 234–238.
[11] U. Groß, S. Rüdiger, E. Kemnitz, Solid State Sci. 9 (2007) 838–842.
[12] S. Lepouter, D. Boyer, A. Pordevin, M. Doubois, V. Briois, R. Mahiou, J. Solid State Chem. 11 (2007) 3049–3057.
[13] P.Y. Jia, J. Lin, M. Yu, J. Lumin. 122–123 (2007) 134–136.
[14] Y.L. Yu, Y.S. Wang, D.Q. Chen, F. Liu, Ceram. Int. 34 (2008) 2143–2145.
[15] Y.C. Yue, Z.G. Hu, C.T. Chen, J. Cryst. Growth 310 (2008) 1264–1267.
[16] Y. Birol, J. Alloy Compd. 443 (2007) 94–98.
[17] X. Wang, J. Zhuang, Q. Peng, Y.D. Li, Inorg. Chem. 45 (2006) 6661–6665.
[18] Z.H. Jia, H.Q. Su, S.H. Feng, C.S. Shi, Chin. Chem. Lett. 12 (2001) 1047–1050.
[19] P. Parhi, J. Kramer, V. Manivannan, J. Mater. Sci. 43 (2008) 5540–5545.
[20] H. Hu, Z.G. Chen, T.Y. Cao, Q. Zhang, M.X. Yu, Nanotechnology 19 (2008) 375702, (9pp).
[21] R.N. Hua, Z.H. Jia, D.M. Xie, C.S. Shi, Chin. Chem. Lett. 13 (2002) 1021–1024.
[22] Y. Kumashiro, S. Ozaki, K. Sato, Y. Kataoka, K. Hirata, T. Yokoyama, S. Nagatani, K. Kajiyama, J. Solid State Chem. 177 (2004) 537–541.
[23] F.T. You, S.H. Huang, D.W. Wang, Y. Huang, J.H. Xu, J. Rare Earths 24 (2006) 396–399.
[24] J.H. Zeng, Z.H. Li, J. Su, L.Y. Wang, R.X. Yan, Y.D. Li, Nanotechnology 17 (2006) 3549–3555.
[25] X. Wang, Y.D. Li, Angew. Chem. Int. Ed. 42 (2003) 3497–3500.
[26] C.Y. Zhao, S.H. Feng, Z.C. Chao, R.R. Xu, C.S. Shi, J.Z. Ni, Chem. Commun. 1641 (1996).
[27] C.Y. Zhao, S.H. Feng, Z.C. Chao, R.R. Xu, C.S. Shi, J.Z. Ni, Chem. Commun. (1997) 945–946.
[28] SMART and SAINT, Siemens Analytical X-ray Instruments, Inc., Madison, WI, 1996.
[29] SHELXTL, Version 5.1, Siemens Industrial Automation, Inc., 1997.
[30] P. Bukovec, N. Bukovec, A. Demšar, J. Therm. Anal. 36 (1990) 1751–1760.
[31] T. Onishi, Y. Yoshioka, J. Surf. Sci. Nanotechnol. 5 (2007) 20–22.